CHIN. PHYS. LETT. Vol. 32, No. 11 (2015) 116802

Improvement of Surface Morphology of Yttrium-Stabilized Zirconia Films Deposited by Pulsed Laser Deposition on Rolling Assisted Biaxially Textured Substrate Tapes *

WANG Meng-Lin(王梦麟), LIU Lin-Fei(刘林飞), LI Yi-Jie(李贻杰)**,

Department of Physics and Astronomy, Shanghai Jiao Tong University, Shanghai 200240

(Received 22 August 2015)

The surface morphology of buffer layer yttrium-stabilized zirconia (YSZ) of $YBa_2Cu_3O_{7-\sigma}$ (YBCO) high temperature superconducting films relies on a series of controllable experimental parameters. In this work, we focus on the influence of pulsed laser frequency and target crystalline type on surface morphology of YSZ films deposited by pulsed laser deposition (PLD) on rolling assisted biaxially textured substrate tapes. Usually two kinds of particles are observed in the YSZ layer: randomly distributed ones on the whole film and self-assembled ones along grain boundaries. SEM images are used to prove that particles can be partly removed when choosing dense targets of single crystalline. Lower frequency of pulsed laser also contributes to a smoother film surface. TEM images are used to view the crystalline structure of thin film. Thus we can obtain a basic understanding of how to prepare a particle-free YSZ buffer layer for YBCO in optimized conditions using PLD. The YBCO layer with nice structure and critical current density of around 5 MA/cm^2 can be reached on smooth YSZ samples.

PACS: 68.55.J−, 68.55.Ln, 68.37.Hk DOI: 10.1088/0256-307X/32/11/116802

YBCO is widely used as a high temperature superconducting material in scientific research. In the process of preparing high quality YBCO thin films, the buffer layer is significant. The most typical buffer layers are CeO_2[1] and yttrium-stabilized zirconia (YSZ),[2] due to their chemical and thermal stability to prevent atomic diffusion and due to their suitable lattice constants for epitaxial growth. Furthermore, there exists a large number of methods to prepare YSZ layers: for example, laser chemical vapor deposition,[3] magnetron sputtering,[4] ion-beam-assisted deposition[5] and pulsed laser deposition.[6] Among them, pulsed laser deposition stands out for its numerous advantages, such as good adherence of stoichiometry to target material.[7] However, one negative point for this technology is that outgrowths and precipitates become more and more during high-temperature deposition, leading to bad quality of thin films.[8]

Precipitates presenting on the surface of a YSZ layer are detrimental to the upper superconducting YBCO layer. For one thing, precipitates may promote exchange of Ni and O atoms between the buffer layer and the substrate by providing a short-cut diffusion passage. Such contamination in composition of YBCO films may limit critical current passing through the superconducting layer. Moreover, the formation of NiO_2 would also have a bad influence on the inner stress of the film,[9] and degrade mechanical properties. For another thing, the coarse surface of films could probably result in the appearance of high-angle grain boundaries, which may lower J_c of the upper YBCO layer.[10] Thus suitable experimental parameters must be found to improve morphology of the YSZ buffer layer.

In this Letter, we study the effect of different physical parameters on morphology of the YSZ layer during pulsed laser deposition. It is hopeful to find key parameters and to realize how these parameters could influence the size and distribution of surface particles. After optimizing the deposition condition for the YSZ buffer layer, we obtain a high-quality YBCO film with better microstructure and larger current density.

The Ni-5 at% (NiW) rolling assisted biaxially textured substrate (RABiTS) tapes made by GMBH (Germany) were used as the substrate in experiment. The tapes were 10 mm in width and 70 μm in thickness, with the rms surface roughness less than 10 nm within region 100 μm×100 μm. This kind of tape had highly ⟨100⟩ cubic texture. The full widths at half maximum (FWHMs) of ω-scan and ϕ-scan were 6° and 7°, respectively. Firstly, CeO_2 was grown as the seed layer on the RABiTS NiW substrate tape by using PLD, details of which would be seen in Ref. [11]. YSZ and YBCO thin films were then deposited on the superior-quality CeO_2/NiW layer by PLD, respectively. Two kinds of YSZ targets of similar stoichiometry ratio while different degrees of crystallinity were used in our experiments.

Film deposition was performed by a Lambda

*Supported by the ITER Project of the Ministry of Science and Technology of China under Grant No 2011GB113004, the Shanghai Commission of Science and Technology under Grant No 11DZ1100402, and the Youth Fund of the National Natural Science Foundation of China under Grant No 11204174.

**Corresponding author. Email: yjli@sjtu.edu.cn

© 2015 Chinese Physical Society and IOP Publishing Ltd

Physik LPX 220 KrF excimer laser (wavelength $\lambda = 248\,\text{nm}$, pulse duration $\tau = 20\,\text{ns}$). The laser focused on the ZrO_2 (Y_2O_3 8%) target with an incident angle of 45°. The target was rotated at a speed of 20 rpm during the ablation to maintain the uniformity of the film.[12] At the beginning, base pressure for PLD chamber was 1×10^{-6} Torr. Then the chamber was filled with a certain amount of oxygen. During YSZ preparation, temperature of the substrate was kept around 800℃. Pulsed laser frequency was altered from 40 Hz to 120 Hz. Moreover, oxygen partial pressure varied from 1 mTorr to 50 mTorr. Then a YBCO layer was deposited on YSZ when O_2 partial pressure was 200 mTorr, laser frequency was 160 Hz and temperature was 1000℃. The structure characterization was carried out by x-ray diffraction (D8 Discover with GADDS, Bruker Advanced X-ray Solutions, Inc.). A high-resolution scanning electron microscope (HRSEM, FEI Sirion 200) and an atom force microscope (AFM, Nanoscope Ⅲ, DI, Santa Barbara, USA) were used to observe the surface morphology.

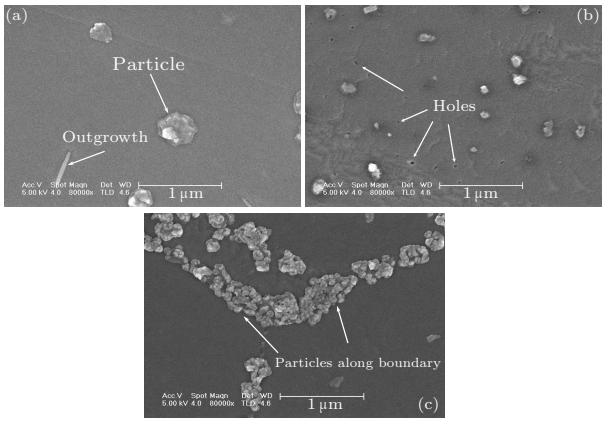


Fig. 1. Four kinds of defects usually seen in the YSZ surface.

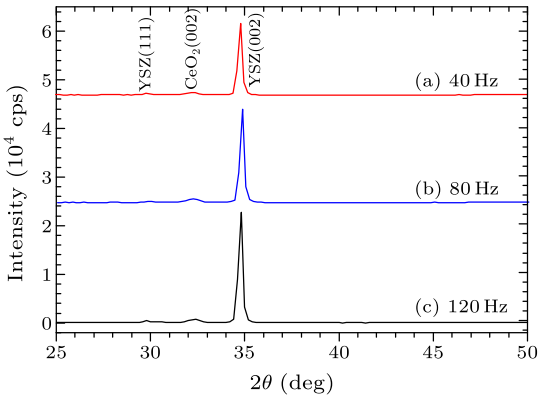


Fig. 2. XRD pattern of samples deposited at lasers of (a) 40 Hz, (b) 80 Hz, and (c) 120 Hz.

Normally, there are four kinds of obvious defects on the surface of the YSZ film: droplet-like particles, needle-like outgrowth, circular holes and particles stacking along grain boundaries,[13] as can be seen in Fig. 1. Among them, needle-like outgrowth and circular holes can be removed by optimizing deposition condition, while droplet-like particles and boundary-grown particles can hardly be eliminated. In this work, we focus on how parameter changes would affect density and diffusion of these particles on the surface of the YSZ film..

YSZ films were prepared at 40 Hz, 80 Hz and 120 Hz, respectively, to study the dependence of surface morphology on laser frequency. The x-ray diffraction curves are shown in Fig. 2. All three samples have sharp peaks at about 35°, indicating YSZ (002).[14] The intensity of YSZ (002) peak increases with higher laser frequency. It is assumed that this may reveal the change of film thickness. No other evident peaks are observed in all studied XRD spectrums. Thus these samples have the good structure and c-axis orientation.

Grain boundaries can be observed clearly on the surface of the YSZ thin film, and it is evident in Fig. 3 that particles prefer to grow on the grain boundaries under lower laser frequency. With frequency of 40 Hz, few droplet-like particles are on the surface and particles along boundaries are more loosely aligned. Oppositely, with higher frequency of 120 Hz, the surface becomes much worse with increasing the number of particles, both on the boundaries and inside grains. In particular, particles randomly distributed increase at a faster rate than others, thus they are more sensitive to the change of laser frequency.

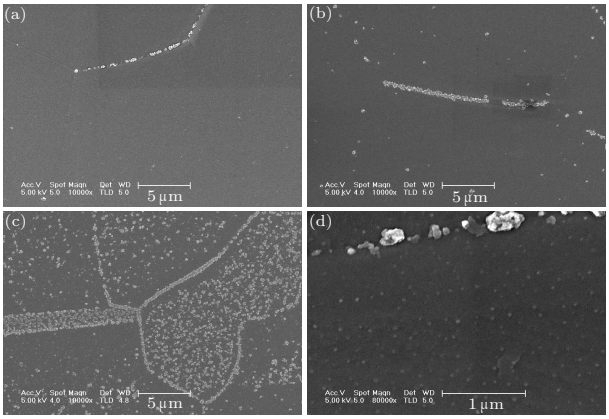


Fig. 3. SEM images of the YSZ film deposited at laser of (a) 40 Hz, (b) 80 Hz, (c) 120 Hz. (d) A magnified photo corresponding to (a).

It should be noted that the frequency of pulsed laser can affect deposition rate on the film surface.[15] When particles arrive at the substrate, they may need time to migrate to suitable positions where the potential energy is lowest. When the frequency is elevated, time duration between two pulses becomes shorter, thus particles are unable to move to the most stable position on the substrate before the next patch of particles arrive. Thus particles can be very near to each other, and clusters and droplets can be much larger.

Unavoidably, more defects appear and the surface becomes rougher. On the contrary, when the appropriate laser frequency is adopted, atoms and ions tend to have enough time to move to the most stable places to nucleate and to form complete crystal structure. Thus the film's homogeneity and integrity would be improved.

Two kinds of commercial targets are used in our experiments. Target 1 is a polycrystalline target with the density of 4.96 g/cm^3. Target 2 is a single-crystal one of 4.9 g/cm^3. Before the experiment, two targets were pre-ablated for 20 min to remove several supernatant layers. Two samples were prepared under the same condition: O_2 partial pressure of 10 mTorr, substrate temperature of 900℃, laser frequency of 120 Hz and laser energy of 280 mJ.

From XRD examination results, we can find that there is only one obvious peak which corresponds to the (002) peak of YSZ. This means that these samples all have the same *c*-axis-oriented structure. The intensity of peaks changes with different targets, revealing that film thickness and lattice constants may not be the same. Also, a small CeO_2 (002) peak is also observed in the diagrams, which reflects the substrate structure. Obviously, the YSZ films inherit the structure of the lower CeO_2 layer. It is mentioned that tiny YSZ(111) peaks can also be seen as well, which may be related to particles and micro cracks on film surfaces. However, their intensity are quite small compared with other peaks.

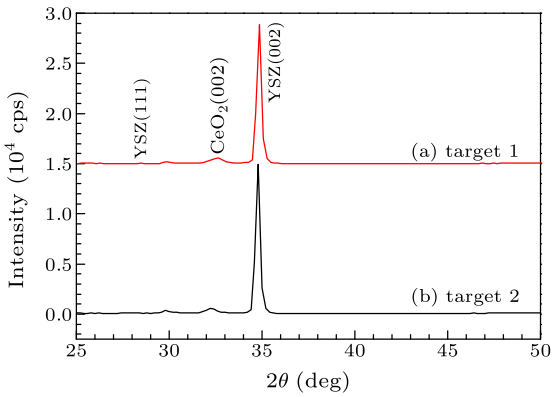


Fig. 4. XRD pattern of samples deposited by (a) target 1 (polycrystalline target) and (b) target 2 (single-crystalline target).

On the SEM microscopy images, we can observe very clearly that there are two kinds of particles on both samples. Some grow along grain boundaries and stack with each other, and others are dispersed randomly on the whole surface. Compared with another sample, films deposited by using single-crystal targets have less and smaller micro cracks and droplets. The surface is much more homogeneous. We can explain such difference from the aspect of target constitution and structure. A single-crystalline target is much more compact and has a higher proportion of single-crystal structure. When it is ablated, particles tend to leave the target surface as a unit containing intact single-crystal substances. As a result, these particles can be deposited on the substrate to form a dense film with less precipitates and visible clusters. Even formed, these precipitates are more likely to hold closely to each other and thus cluster size can be very small.

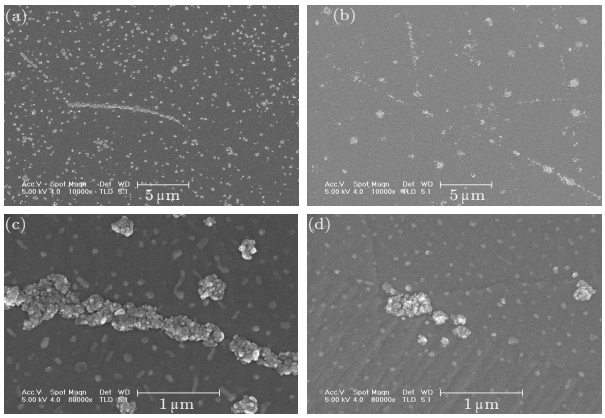


Fig. 5. SEM images of the YSZ film deposited by (a) target 1 (polycrystalline target), (b) target 2 (single-crystalline target), and (c) and (d) are magnified photos corresponding to (a) and (b), respectively.

On the contrary, the polycrystalline target is looser with particles of larger grain size. Usually a larger size plume can be formed when the polycrystalline target is ablated by the laser beam. At the same time, these ablated particles could react with atoms and ions in ambient gas and form larger clusters. Thus when they arrive at the substrate, more particles would deposit at the grain boundaries and even attract many other larger ones to locate at the same place or nearby. To those landing inside the grains, sizes of droplets and clusters are much larger as well. More particles in a larger plume can also lead to high density dispersion of particles on the film surface. Thus the deposited film is much worse compared with the ones previously mentioned.

As mentioned before, the purpose of obtaining a smooth YSZ layer is to lay the foundation for a high quality YBCO superconducting layer. Here one YSZ sample (Fig. 5(a)) under an optimized deposition condition (40 Hz laser frequency and single-crystal target) and one YSZ sample (Fig. 5(b)) under the normal condition (80 Hz and polycrystalline target) are chosen as the substrates to further deposit YBCO. The YBCO layer is prepared by using the following experiment parameters: O_2 partial pressure of 200 mTorr, substrate temperature of 1050℃, laser frequency of 160 Hz and laser energy of 300 mJ. Figure 6 is the AFM images of the YSZ samples (Figs. 6(a) and 6(b)) and the YBCO samples (Figs. 6(c) and 6(d)) corresponding to the samples shown in Figs. 6(a) and 6(b).

Large precipitates and grain boundaries can be seen in the YSZ sample (Figs. 6(b)). Obviously, the YBCO sample (Figs. 6(c)) deposited on the nice YSZ surface has much less particles than the YBCO sample (Figs. 6(d)). Thus we can conclude that the smooth surface of the YSZ layer is beneficial for the improvement of surface quality of the upper YBCO layer. Then quality of the sample shown Figs. 6(c) is characterized by TEM, SEM, XRD and the standard four-pole I–V measurement.

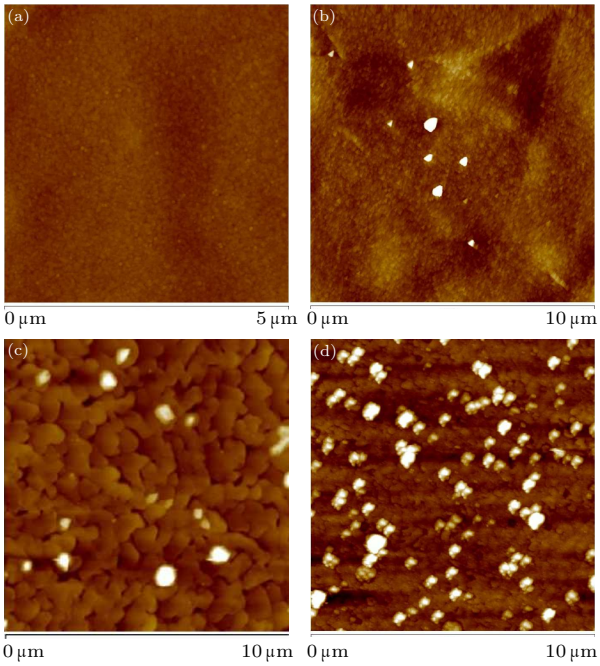


Fig. 6. AFM images of optimized surface (a) and normal surface (b) of the YSZ samples. (c) and (d) Surface morphology images of YBCO layers deposited on (a) and (b), respectively. The data of rms roughness R_q of (a), (b), (c) and (d) are 1.21 nm, 4.2 nm, 31.4 nm and 42.7 nm, respectively.

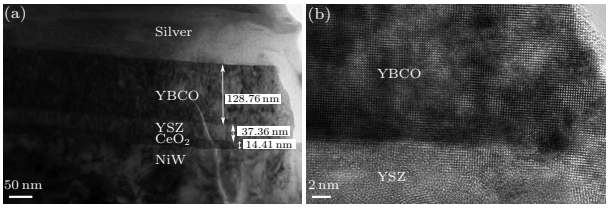


Fig. 7. (a) TEM images of the NiW/CeO_2/YSZ/YBCO multilayer structure in our representative sample. (b) TEM images of the YSZ/YBCO layer interface and crystalline structure.

The layer structure can be viewed clearly from the following cross-sectional TEM image (Fig. 7.(a)). There are five layers from bottom to top: NiW/CeO_2/YSZ/YBCO/silver. The uppermost silver coating is a covering layer to keep the tape from air contamination. They are not of definite ordered structure. NiW is textured metal template. The intermediate triple layers CeO_2/YSZ/YBCO all have the tendency to grow along c-axis vertical to the surface, and upper layers may inherit the c-axis texture architecture of lower layer. The boundary of these layers can be seen clearly. Some of the layers' thickness are marked in Fig. 7.

Figure 7(b) is the magnified version of Fig. 7(a) to see more clearly into the interface between YSZ and YBCO. From this picture, crystal lattice can be seen distinctly and they are arranged to each other closely and regularly. The diameters of crystalline lattice of YSZ and YBCO are similar and in numeric order of about 0.1 nm. Admitting that they have slight difference in growth orientation, both films have almost the same growth direction in c-axis vertical to the surface, corresponding to our success in epitaxial deposition of YBCO layer. There is no obvious interface layer like tens of layers thick seen in the image, which may be attributed to YSZ layer's smooth and clear surface.

The structure of this YBCO layer can be examined by XRD θ and ϕ scan. Only $(00n)$ peaks can be seen, which proves that they are all c-axis orientated. According to our ϕ measurement, the in-plane texture value is 3.41, showing that the YBCO layer has a good preferred orientation inside the a–b plane. From the current–voltage curve, we can see that the critical current of the YBCO layer is about 60 A, and the critical current density is around 5 MA/cm^2. Also, this sample possesses nice surface morphology that may lead to high current.

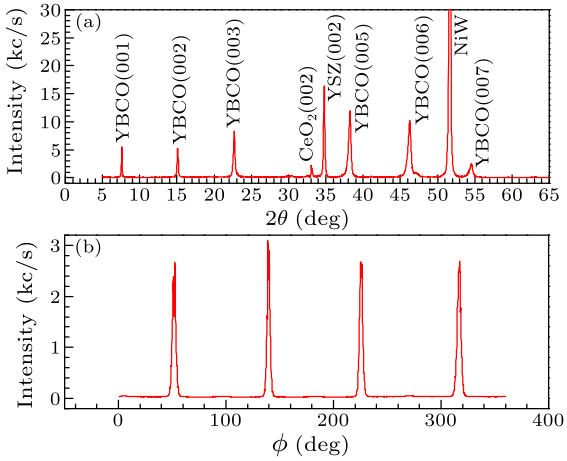


Fig. 8. XRD curves of the YBCO samples. The upper one is the 2θ curve. The lower one is the ϕ scan curve and the texture value is 3.41.

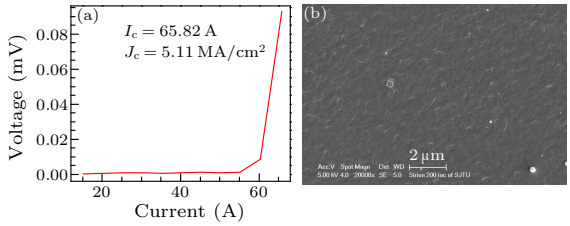


Fig. 9. The I–V curve by the standard four-pole method and the SEM image of the YBCO sample.

In summary, particles distributed randomly and

assembling along grain boundaries are observed in the surface of YSZ layers deposited by PLD. Adopting single-crystalline targets can reduce the presence of these particles. Moreover, lower frequency of the pulsed laser also contributes to a smooth surface. Thus the high-quality YSZ thin film with pure *c*-axis orientation and smooth surface morphology can be prepared. Furthermore, the YBCO layer of good biaxial texture and high current can be achieved on the typical YSZ sample with a smooth surface.

References

[1] Muroga T, Iwai H, Yamada Y, Izumi T, Shiohara Y, Iijima Y, Saito T, Kato T, Sugawara Y and Hirayama T 2003 *Physica* C **392** 796

[2] Savvides N and Gnanarajan S 2003 *Physica* C **387** 328

[3] Kimura T and Goto T 2003 *Mater. Trans.* **44** 421

[4] Hidalgo H, Reguzina E, Millon E, Thomann A L, Mathias J, Boulmer-Leborgne C, Sauvage T and Brault P 2011 *Surf. Coatings Technol.* **205** 4495

[5] Chudzik M P, Erck R and Lanagan R 1999 *IEEE Trans. Appl. Supercond.* **9** 2

[6] Infortuna A, Harvey A S and Gauckler L J 2008 *Adv. Funct. Mater.* **18** 127

[7] Trtik V, Jeinek M and JastrabIk L 1995 *Laser Methods Surf. Treatment Modification: ALT' 94 International Conference* (Washington, 1–3 March 1995) p 79

[8] Blank D H A, Rijnders A J H M, Roesthuis F J G, Ouden G D and Rogalla H 1996 *Appl. Surf. Sci.* **96** 685

[9] Dhaka A, Sander D, Meyerheim H L, Mohseni K, Soyka E, Kirschner J, Adeagbo W A, Fischer G, Ernst A and Hergert W 2011 *Phys. Rev.* B **84** 195441

[10] Klie R F, Buban J P, Varela M, Franceschetti A, Jooss C, Zhu Y, Browning N D, Pantelides S T and Pennycook S J 2005 *Nature* **435** 475

[11] Li Y, Zhang Z, Liu L, Ye Q and Zheng H 2009 *IEEE Trans. Appl. Supercond.* **19** 3295

[12] Ceresara L, Fuso F, Arimondo E and Scardi P 1997 *Agosto-Settembre* **19** 1033

[13] Wang Y, Liu L, Liu H, Song X, Hong D, Xu D, Zhu S and Li Y 2012 *J. Supercond. Novel Magn.* **25** 11

[14] Fork D K, Fenner D B, Connell G A N, Phillips J M and Geballe T H 1990 *Appl. Phys. Lett.* **57** 1137

[15] Golovchanskiy I A, Fedoseev S A and Pan A V 2013 *J. Phys. D: Appl. Phys.* **46** 215502